Rheology, Structure, and Properties of Ethylene–Vinyl Acetate/Metallocene-Catalyzed Ethylene–α-Olefin Copolymer Blends

Marianna Kontopoulou, Leo C. Huang

Department of Chemical Engineering, Queen's University, Kingston, Ontario K7L 3N6, Canada

Received 8 October 2003; accepted 27 April 2004
DOI 10.1002/app.20913
Published online in Wiley InterScience (www.interscience.wiley.com).

ABSTRACT: The rheology, morphology, thermal, mechanical, and adhesive properties of blends containing ethylene–vinyl acetate and metallocene-catalyzed ethylene–α-olefin copolymers, containing butene and octene comonomers, were investigated. On the basis of the thermal and rheological properties and scanning electron microscopy observations, we deduced that these blends were immiscible, both in the solid and melt states over the whole range of compositions. Rheological properties were correlated to blend morphology with the Palierne emulsion model. The butene-based blends had better mechanical properties, which was attributed to their finer morphology, lower interfacial tension, and better adhesive properties. © 2004 Wiley Periodicals, Inc. J Appl Polym Sci 94: 881–889, 2004

Key words: metallocene polyethylene; blends; adhesives

INTRODUCTION

Vinyl acetate (VAc)/ethylene copolymers, often referred to as ethylene-vinyl acetate (EVA) are thermoplastics that are synthesized by the copolymerization of ethylene and VAc. Their thermal and rheological properties vary substantially as a function of VAc content,[1–3] which allows for the tailoring of their properties to render them suitable for diverse applications, such as hot-melt adhesives, films, and foams.

EVA is often compounded with other polyolefins, such as polypropylene and polyethylene, forming thermodynamically immiscible but mechanically compatible blends. Blends of EVA with low-density polyethylene have been the focus of many studies[4–6] because of their extensive use in several practical applications, including packaging films, extruded foam profiles, sheets for automobile parts, and electric cable insulation. The rheological properties and processability of blends of EVA with low-density polyethylene and metallocene-catalyzed polyethylene were studied recently by Peón and coworkers.[7–9] Blends of EVA with metallocene catalyzed ethylene–α-olefin copolymers (ECs) for film applications were also reported.[10] EVA has also been used for the impact modification of polypropylene[11–13] and in blends with EPDM.[14–16]

In this study, we examined the rheological and solid-state properties of binary blends containing EVA and metallocene-catalyzed ultra-low-density ECs, with particular focus on the effect of the comonomer type (butene vs octene) contained in the copolymer. Because a potential end use of these blends is in hot-melt adhesives formulations, special attention was paid to their adhesive properties.

EXPERIMENTAL

Materials and blend preparation

Blends of an EVA with an ethylene–octene copolymer (EOC) and an ethylene–butene copolymer (EBC) were prepared with a Berstorff ZE-40A 43 mm corotating twin-screw extruder (Florence, KY) with a length-to-diameter ratio of 40:1, equipped with a Gala pelletizer (Gala Industries, Inc., Eagle Rock, VA). The extruder was operated at 150 rpm, with an output rate of 18 kg/h. The extrusion temperatures ranged from 150°C in the feeding zone to 190°C at the die, and the melt temperature ranged between 223 and 235°C, depending on the blend composition. A series of blends containing 25, 50, and 75% EVA were prepared. The pure components were similarly compounded to provide control materials for comparative evaluations. The polymers used in this study had comparable molecular weights, which made them suitable for hot-melt adhesive formulations. The properties of the pure components are summarized in Table I.

Correspondence to: M. Kontopoulou (kontop@chee.queensu.ca).

Contract grant sponsor: Materials and Manufacturing Ontario.
Contract grant sponsor: AT Plastics, Inc.

TABLE I
Material Properties

Resin	Comonomer type	Melt flow index (g/10 min)	Melting temperature (°C)	Density (kg/m^3)
EVA	VAC	9.3	74	949
EBC	Butene	11.2	67	880
EOC	Octene	8.6	63	870

Thermal and rheological properties

A controlled stress rheometer (ViscoTech by Reologica Instruments AB, Lund, Sweden) with parallel plates (20 mm in diameter) was used in the oscillatory mode to measure linear viscoelastic properties, with a gap of 1.5 mm. All measurements were carried out under a nitrogen atmosphere to limit degradation and the absorption of moisture.

The thermal properties were evaluated with a Seiko DSC 2209, by Seiko Instruments, Inc., purchased from Thermo Haake (Madison, WI). Samples weighing 10 mg were placed in an aluminum pan and heated to 150°C to eliminate the thermal history of the material. Subsequently, the samples were cooled to −50°C at a rate of 10°C/min and heated for a second time to 150°C at a rate of 5°C/min. Melting temperatures and heats of fusion were recorded during the second heating sequence.

Dynamic mechanical analysis (DMA)

The temperature dependence of the elastic modulus (G'), loss modulus (G''), and loss tangent (tan δ) was recorded with the controlled stress rheometer in torsion between −95 and 60°C. The frequency (ω) was set to 1 Hz, the strain was 0.1%, and the heating rate was 5°C/min. Glass-transition temperatures were obtained from the peak of the tan δ curve.

Scanning electron microscopy (SEM)

We prepared specimens for SEM by heating the polymers to 190°C and immediately quenching them in cold water to freeze their morphology. The samples were freeze-fractured with liquid nitrogen, gold coated, and observed with a Philips XL 3°CP scanning electron microscope with a beam power of 20 kV. Images were analyzed with SigmaScan Pro Image Analysis software (Leesburg, VA). At least 250 particles were used to calculate their average diameter.

Optical properties

Tapes of approximately 4 mm in thickness were produced for optical property characterization with a 1.5-in. Stirling extruder equipped with a 4-in. width coat-hanger die and chilled rolls. The extruder was operated at 30 rpm, the temperature was varied from 140°C in the feeding zone to 160°C in the die, and the melt temperature was 160°C. The chilled rolls were maintained at 35°C.

A Gardner XL-210 Hazegard system (BYK-Gardner, Columbia, MD) was used to perform haze measurements on the tapes according to ASTM D 1003-97. A Gardner Glossgard system 45 was used for gloss measurements, according to ASTM D 2457-70. In both tests, the average of five measurements is reported.

Tensile properties

A tabletop injection molder from Mining & Chemical Products, Inc. (Willingborough, United Kingdom) was used to produce the specimens for the tensile tests (Type III according to ASTM D 638M). A Monsanto Tensometer 10 (St. Louis, MO) was used to carry out the tensile tests in accordance to ASTM D 638M at speeds of 50 and 500 mm/min. Five trials were performed per sample.

T-peel adhesion

Blends for the T-peel tests were prepared by roll milling at 100°C. Approximately 100 g of the dry-blended material was added to the rolls, which were being operated initially at a speed of 10–15 rpm and subsequently at 25–30 rpm. All of the samples for T-peel testing were prepared according to ASTM D 1928-96. We prepared the plaques by placing 20 g of polymer resin and five sheets of Mylar between two aluminum sheets in a 175 ×160 mm picture-frame mold and compression molding at 165°C with a Wabash press (Wabash, IN). Samples were subjected to low pressure (~15 psi) for 5 min and subsequently to higher pressure (~1500 psi) for another 5 min and cooled to room temperature. A die (150 × 25 mm) was used to cut out the test specimens.

T-peel tests were performed in accordance with ASTM D 1876-93 with an Instron 4464 (Canton, MA) tensile testing machine. Three specimens were tested for each blend composition. A crosshead speed of 280 mm/min with grips approximately 12 mm apart and a load of 2 kN were used for a sample width of 25 mm.

RESULTS AND DISCUSSION

Viscoelastic properties

Figures 1 and 2 depict the complex viscosity (η^*) and G' values of the EVA/EBC and EVA/EOC blends at 190°C. Discrete relaxation spectra were obtained by fitting G' and G'' with the generalized Maxwell model, as shown in eq. (1). The respective fits are shown in Figures 1(b) and 2(b):

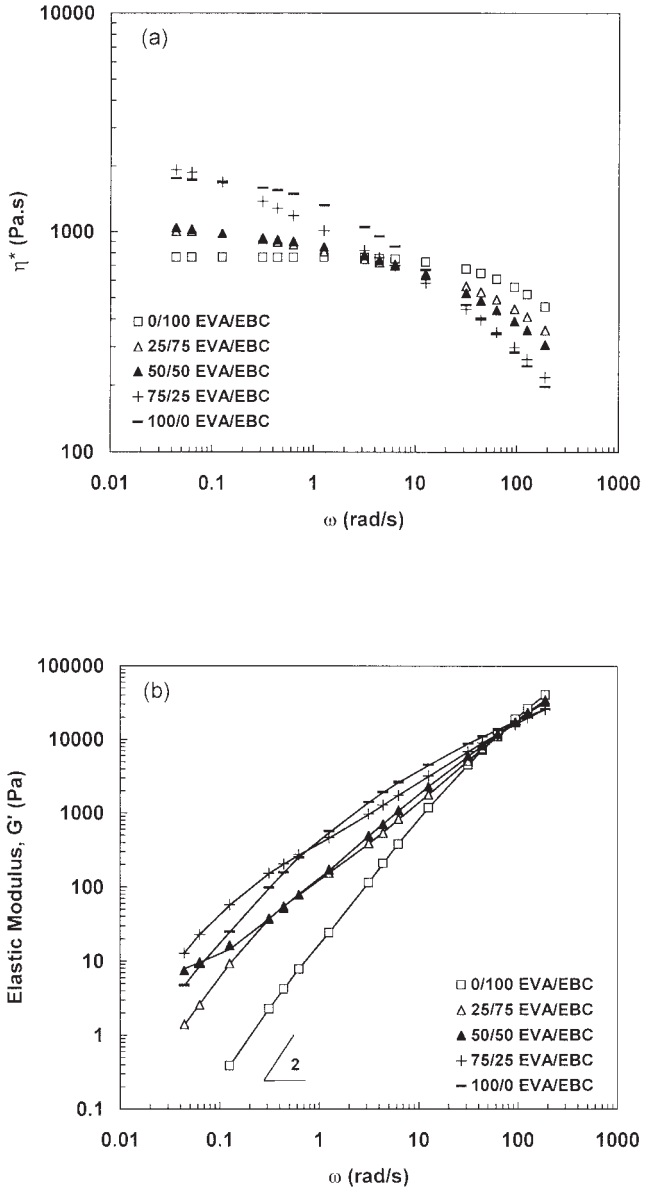

Figure 1 Viscoelastic properties of EVA/EBC blends at 190°C: (a) η^* and (b) G', as a function of ω.

$$G'(\omega) = \sum_i G_i \frac{\omega^2\lambda_i^2}{1 + \omega^2\lambda_i^2} \qquad (1)$$

$$G''(\omega) = \sum_i G_i \frac{\omega\lambda_i}{1 + \omega^2\lambda_i^2}$$

Zero-shear viscosity (η_0), steady-state compliance (J_S^0), and terminal relaxation times (λ's) were calculated from the discrete relaxation spectra according to eqs. (2)–(4)[17] and are summarized in Table II:

$$\eta_0 = \sum_n G_i\lambda_i \qquad (2)$$

$$J_S^0 = \frac{\Sigma G_i\lambda_i^2}{(\Sigma G_i\lambda_i)^2} \qquad (3)$$

$$\lambda \cong \eta_0 J_S^0 \qquad (4)$$

Master curves were constructed with the time–temperature superposition principle, where α_T and b_T are the horizontal and vertical shift factors, respectively:[18]

$$b_T G'(\alpha_T\omega, T) = G'(\omega, T_o)$$
$$b_T G''(\alpha_T\omega, T) = G''(\omega, T_o) \qquad (5)$$

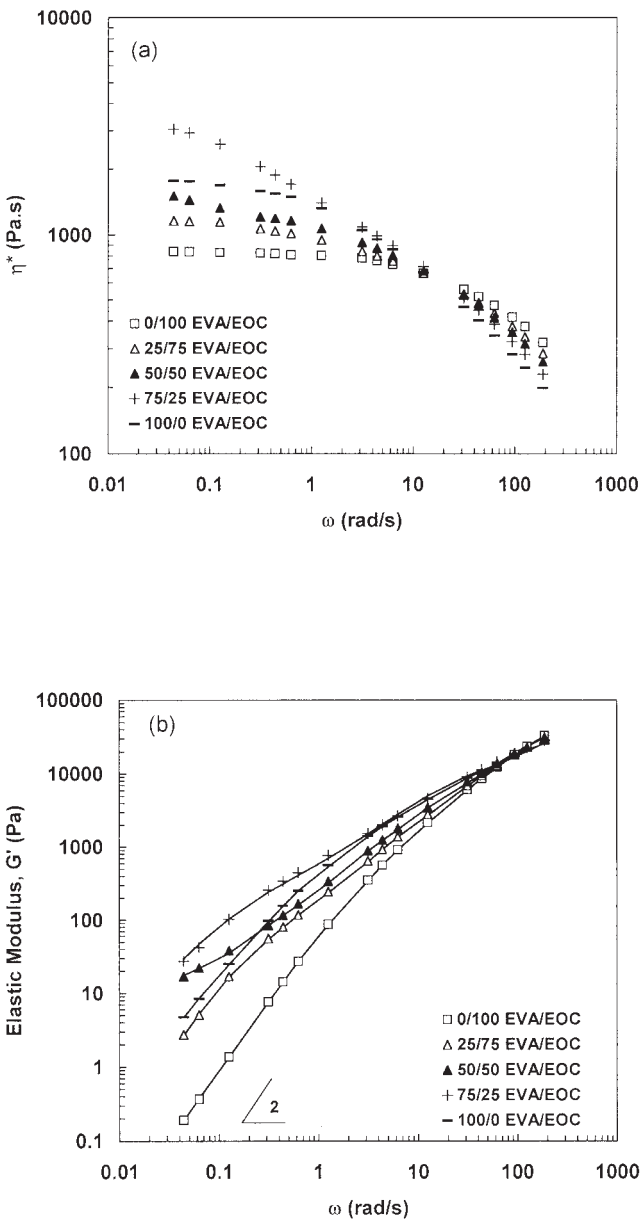

Figure 2 Viscoelastic properties of EVA/EOC blends at 190°C: (a) η^* and (b) G', as a function of ω.

TABLE II
Viscoelastic Parameters at 190°C

Blend composition	η_0 (Pas)		λ (s)		$J_S^0 \times 10^3$ (Pa^{-1})		ΔE (kJ/mol)	
	EVA/EBC	EVA/EOC	EVA/EBC	EVA/EOC	EVA/EBC	EVA/EOC	EVA/EBC	EVA/EOC
0/100	778	851	0.03	0.12	0.02	0.14	22.8	44.1
25/75	1025	1270	1.14	1.13	1.11	0.89	30.9	44.8
50/50	1380	2208	12.50	15.10	9.08	6.84	40.8	42.9
75/25	2099	3493	3.80	6.60	1.81	1.89	46.7	45.5
100/0	1873	1873	1.47	1.47	0.78	0.78	46.7	46.7

where T is the temperature and T_o is a reference temperature.

Horizontal activation energies were calculated by the application of an Arrhenius-type dependence to α_T [eq. (6)] and are shown in Table II:

$$\alpha_T = \exp\left[\frac{\Delta E}{R}\left(\frac{1}{T} - \frac{1}{T_o}\right)\right] \quad (6)$$

where ΔE is the flow activation energy, R is the ideal gas constant, T_o is the reference temperature, and T is the actual temperature. b_T closely followed the well-known relation:[18]

$$b_T = \frac{T_o \rho_o}{T \rho} \quad (7)$$

where ρ and ρ_o are the densities at T and T_o, respectively. We assumed that in the temperature range under consideration, $\rho/\rho_o = 1$.

The η_0 values of the blends showed positive deviation behavior with respect to additivity, as demonstrated in Figure 3. Similar behavior has been noted previously for many immiscible polyolefin blends.[19] At high frequencies (corresponding to high shear rates), the addition of EVA to both ECs clearly lowered their viscosity values, and the additivity rule was followed closely.

The viscoelastic parameters summarized in Table II revealed that in terms of the pure components, EVA was the most elastic because it had the highest values of relaxation time and elastic compliance due to the large amount of long-chain branching it contained. EBC was the least elastic because it did not contain any long-chain branching. The J_S^0 and λ values of the blends showed strong positive deviation behavior, suggesting that they were significantly more elastic than the pure materials. The values of the viscoelastic properties of the EOC-based blends and their activation energies (Table II) were higher because of the long-chain branching contained in the octene-based copolymer. Long-chain branching favored shear thinning, which rendered the viscosities of EOC and EOC-rich blends lower at high frequencies (see also Fig. 3) and thus implied improved processability.

On closer examination of the G' values shown in Figures 1(b) and 2(b), it is obvious that even though the pure components approached the terminal flow region where $G' \propto \omega^2$, all of the blends displayed significant elasticity enhancement compared to additivity and deviation from terminal flow at low frequencies. Increased elasticity at low frequencies is commonly observed in immiscible polymer blends and is attributed to the deformability and relaxation of the droplets that are suspended inside the matrix.[20,21]

The shift in the viscoelastic response of blends toward longer relaxation times could be better demonstrated with plots of the weighted relaxation spectra [$\lambda H(\lambda)$] as a function of log λ.[21,22] The relaxation spectrum [$H(\lambda)$] was calculated from the experimental G' and G'' data, according to the expressions in eq. (8), with the method proposed by Ferry:[23]

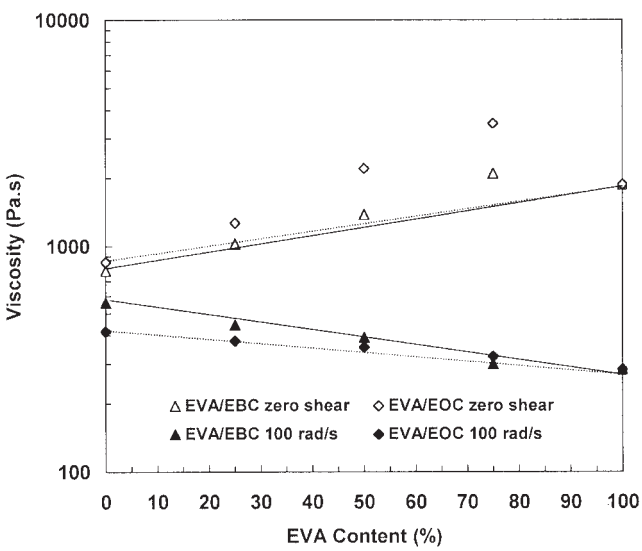

Figure 3 η_0 and viscosity at 100 rad/s as a function of EVA content at 190°C. The lines depict the rule of additivity for EVA/EBC and EVA/EOC.

$$G'(\omega) = \int_{-\infty}^{\infty} [H(\lambda)\omega^2\lambda^2/(1 + \omega^2\lambda^2)]\, d(\ln \lambda)$$

$$G''(\omega) = \int_{-\infty}^{\infty} [H(\lambda)\omega\lambda/(1 + \omega^2\lambda^2)]\, d(\ln \lambda) \qquad (8)$$

As expected for immiscible blends, peaks corresponding to the individual components were seen in the blend spectra shown in Figure 4; however, the location of the peaks appeared shifted toward longer relaxation times. The spectra of the pure EBC and EOC themselves had two peaks, possibly because of inhomogeneities in the molecular structure because of the presence of branching.

The observed viscoelastic properties could be correlated to blend morphology, as discussed in the next section.

Blend morphology

Droplet-matrix morphology was observed for the 25/75 and 75/25 blend compositions of both systems, as presented in Figure 5. The corresponding average particle sizes are summarized in Table III. For all of the blends, the minor phase was homogeneously dispersed, and the particle size distribution was relatively narrow, with the exception of the 25/75 EVA/EOC composition. The images for the 50/50 compositions of both systems appeared relatively homogeneous, with no sufficient contrast to distinguish between the two phases. Probable explanations for this observation could be either that the size of the dispersed phase was very small, resulting in very fine morphology, or that co-continuous morphologies were present. The latter is more plausible as these compositions were likely close to phase inversion and co-continuous morphologies have been reported in similar blends previously.[10] To verify the existence of two phases at this composition, the optical properties, such as haze and gloss, of the films were evaluated. The fact that haze reached a maximum and, correspondingly, that gloss was minimum at this composition, as seen in Figure 6 for the EVA/EOC blends, corroborated our assumption that two phases were present in the blend but could not be detected by SEM because of low contrast.

As shown in Table III, the morphology of the 25/75 EVA/EBC blend was finer than that of the respective EVA/EOC blend, even though the viscosity ratio (defined as $\eta_{dispersed}/\eta_{matrix}$ where $\eta_{dispersed}$ and η_{matrix} are the viscosities of the dispersed and matrix phases respectively, calculated at a nominal shear rate of 100 s^{-1}) of the EVA/EOC blend was closer to 1. This translated to a higher value of interfacial tension between EVA and EOC, as estimated with the Palierne model.[24,25] A typical fit of the G' as a function of ω, obtained by the fitting of the Palierne model to the experimental data for the EVA/EOC 25/75 composition at 190°C, is shown in Figure 7. The interfacial tension values obtained for all of the compositions are summarized in Table III.

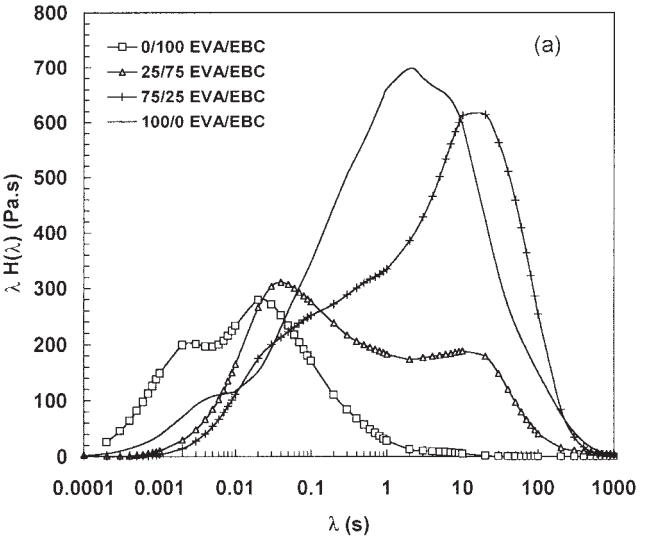

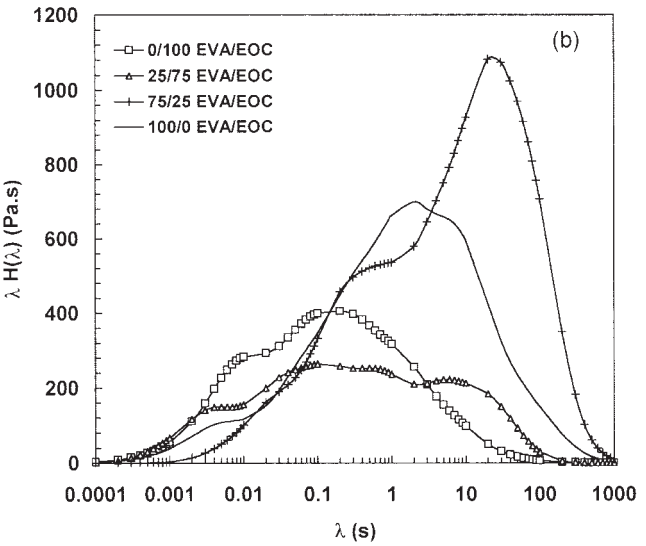

Figure 4 Weighted relaxation spectra of pure materials and their blends at 190°C: (a) EVA/EBC system and (b) EVA/EOC system.

Thermal properties

Differential scanning calorimetry (DSC) endotherms of the pure components and their blends are shown in

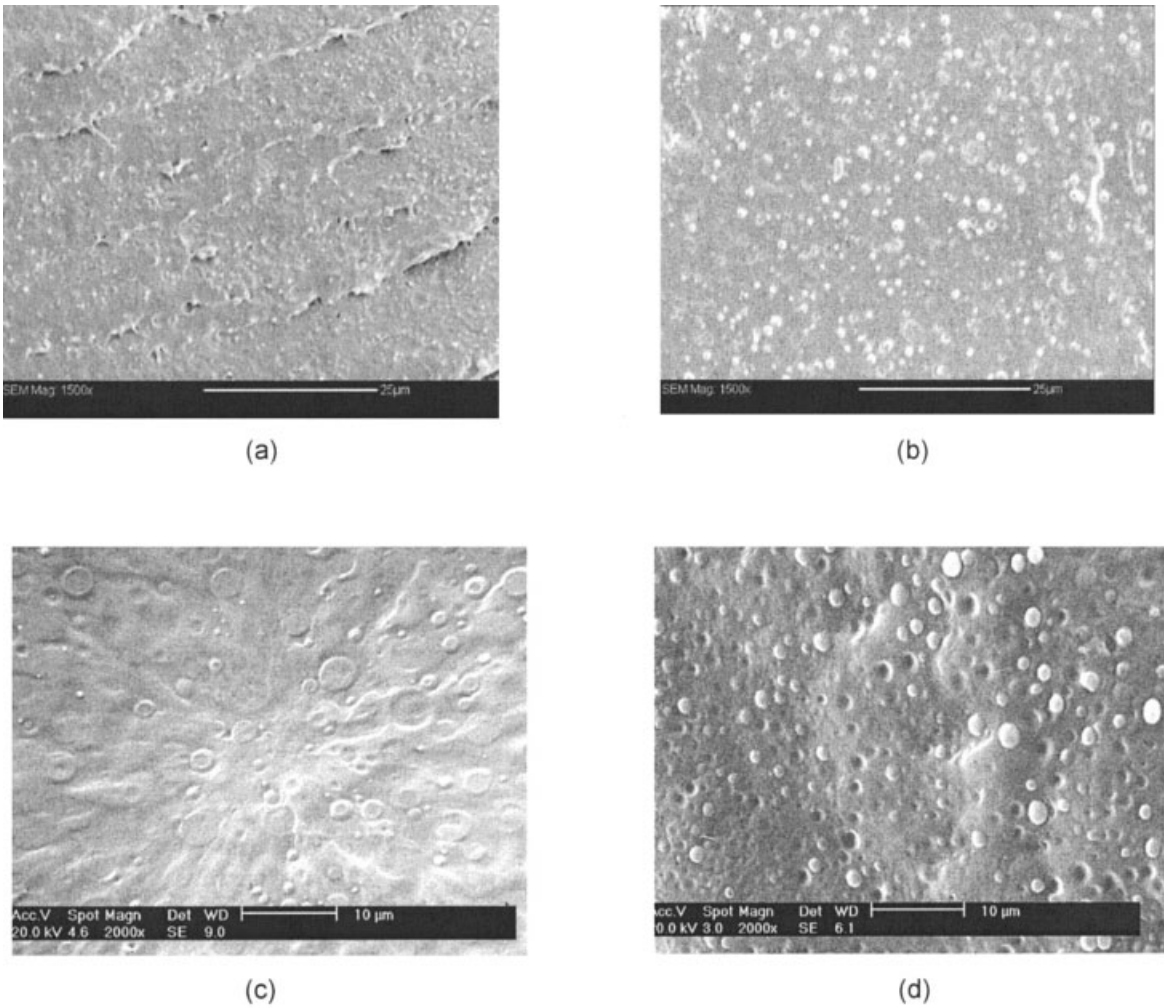

Figure 5 SEM images of the blends: (a) 25/75 EVA/EBC, (b) 75/25 EVA/EBC, (c) 25/75 EVA/EOC, and (d) 75/25 EVA/EOC.

Figure 8(a,b). Both pure materials displayed broad melting endotherms, representative of the high VAc content of the EVA[1] and the very low density of the ethylene copolymers.[26] The pure EOC displayed two peaks, in agreement with the observations of Simanke et al.[26] This may have been because the octene comonomer formed a separate crystalline phase. This peak persisted in the DSC endotherms of the EOC-based blends.

TABLE III
Viscosity Ratio, Particle Size, and Interfacial Tension Estimated from the Palierne Model at 190°C

Blend	Viscosity ratio	Number-average diameter (μm)	Interfacial tension (mN/m)
EVA/EBC 25/75	0.5	0.80 ± 0.21	0.7
EVA/EBC 75/25	2.0	1.04 ± 0.32	0.6
EVA/EOC 25/75	0.7	2.73 ± 1.00	1.4
EVA/EOC 75/25	1.5	1.48 ± 0.32	0.6

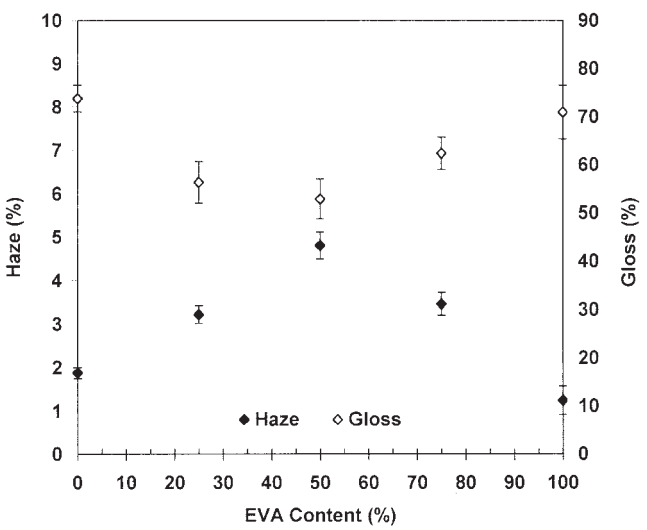

Figure 6 Optical properties of EOC blends as a function of EVA content.

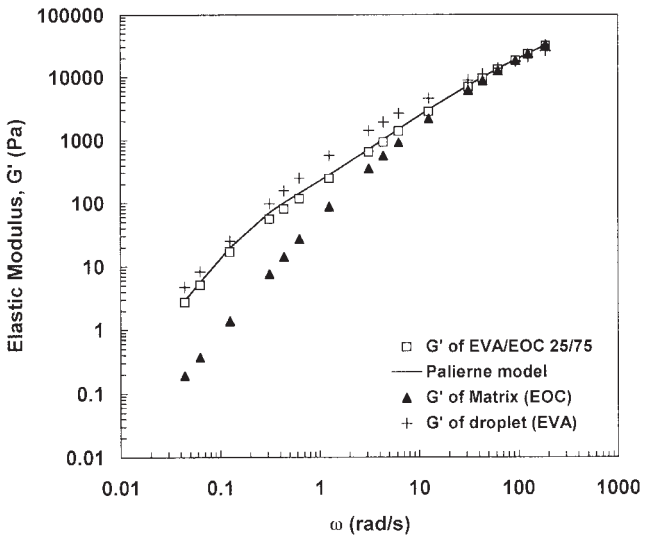

Figure 7 Palierne model fit for the 25/75 EVA/EOC blend at 190°C.

The slight shifts seen in the melting peaks of all of the blends may have been due to the occurrence of co-crystallization and/or dilution effects because of the proximity of the melting points of the two materials. The proximity between the melting points made it impossible to resolve any potentially existing individual peaks corresponding to EVA and the ECs.

The glass-transition temperatures of the pure materials, determined from the peaks of the tan δ versus temperature curves, shown in Figure 9(a,b), were −27°C for EVA, −43.5°C for EOC, and −60°C for EBC. The absence of shifts in the peaks in the DMA traces of the blends confirmed that they were immiscible. The 25/75 EVA/EBC blend composition posed an exception. This blend had very fine morphology, as evidenced in Table III and Figure 5, and partial miscibility in the amorphous phase may have existed in this composition.

Mechanical properties

Table IV summarizes the tensile properties of EVA, EBC, EOC, and their blends. Among the pure materials, the butene-based EBC exhibited the best tensile properties, followed by the EOC. All of the EBC-based blends had better tensile properties than those containing EOC. This may have been due to the better mechanical properties of the neat EBC compared to EOC. On the basis of morphological observations, we suggest that EVA and EBC are more compatible, translating into better mechanical properties.

Higher testing speeds had a detrimental effect on the properties of EBC and its blends, whereas the effect was less prominent in the case of EOC-based materials and was negligible for pure EVA. This behavior may have been associated with the polymer structure. The more long-chain branching there was in the polymers, the least they seemed to be affected by the speed of testing. These results imply that selection of the optimum blend formulation depended on the intended application and the expected speeds of deformation that the materials may have experienced.

DMA revealed that in terms of the pure materials, EBC was the stiffest above −10°C, followed by EOC and EVA, whereas at lower temperatures, EVA was the stiffest [Fig. 10(a,b)]. Generally, the G' values of the EBC-based blends were higher than those of the EOC-based blends, and most of the blends displayed synergistic effects, with their G' values higher than those of the pure materials in the entire temperature range.

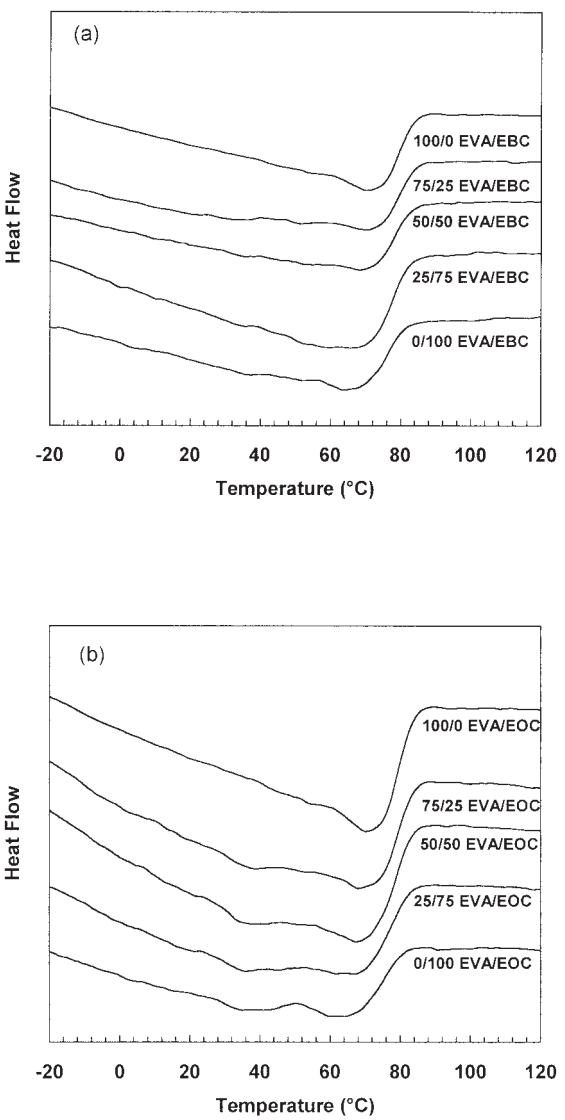

Figure 8 DSC endotherms of pure materials and their blends: (a) EVA/EBC system and (b) EVA/EOC system.

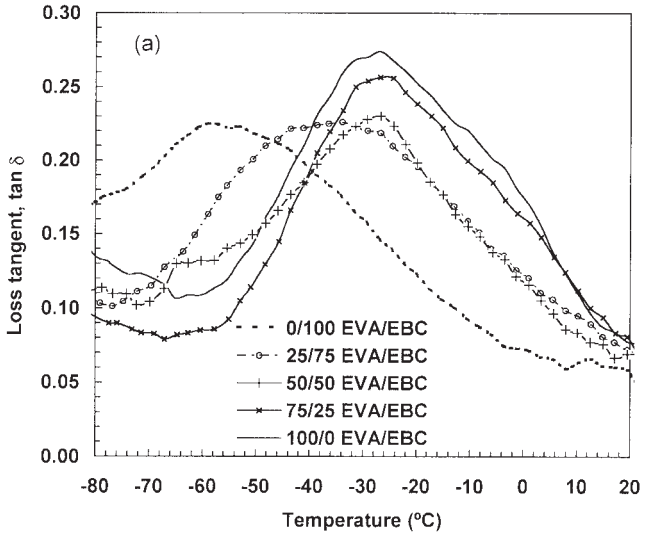

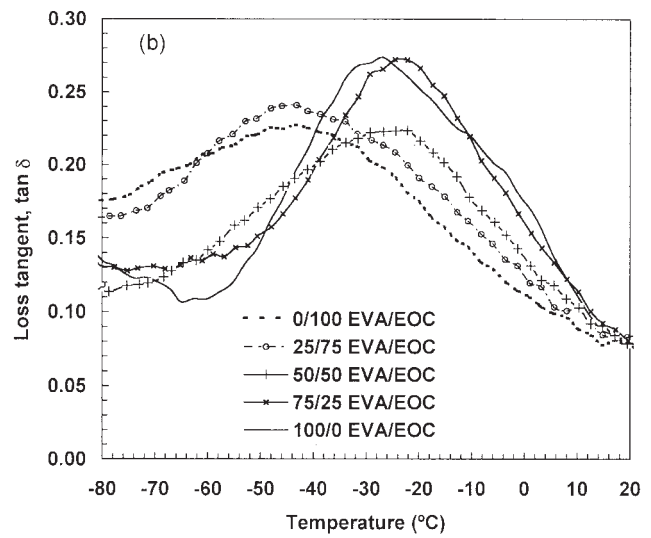

Figure 9 Tan δ, as a function of the temperature of pure materials and their blends: (a) EVA/EBC system and (b) EVA/EOC system.

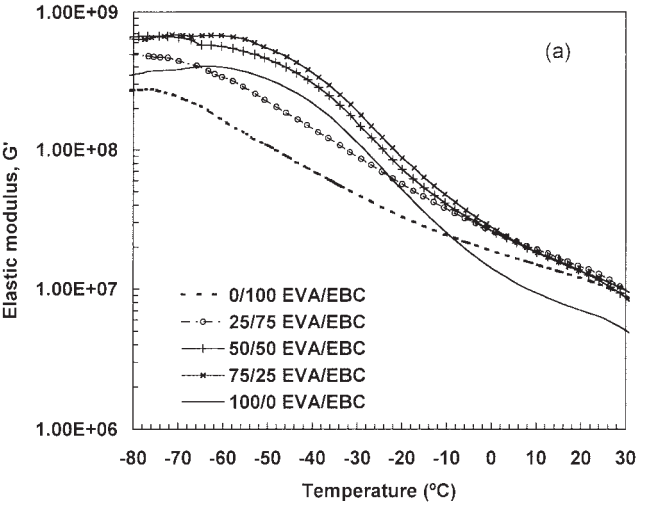

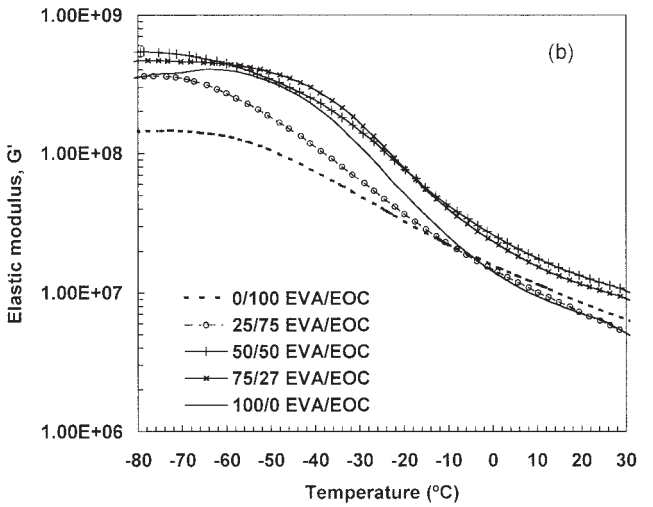

Figure 10 G' as a function of the temperature of pure materials and their blends: (a) EVA/EBC system and (b) EVA/EOC system.

TABLE IV
Tensile Properties at Two Testing Speeds

	Stress at break (MPa)		Elongation at break (%)	
Material	50 mm/min	500 mm/min	50 mm/min	500 mm/min
EVA/EBC				
0/100	8.93 ± 1.02	5.96 ± 0.40	1161 ± 53	286 ± 21
25/75	8.57 ± 0.61	5.88 ± 0.26	956 ± 96	239 ± 12
50/50	8.20 ± 0.77	6.26 ± 0.40	868 ± 39	195 ± 31
75/25	6.77 ± 0.21	6.30 ± 0.07	553 ± 49	149 ± 12
100/0	5.97 ± 0.59	5.64 ± 0.11	428 ± 20	340 ± 34
EVA/EOC				
0/100	6.33 ± 0.30	4.43 ± 0.29	1079 ± 35	939 ± 42
25/75	6.43 ± 0.41	4.60 ± 0.20	967 ± 55	530 ± 48
50/50	5.80 ± 0.17	4.90 ± 0.07	578 ± 41	526 ± 28
75/25	6.23 ± 0.21	5.40 ± 0.17	394 ± 14	364 ± 23
100/0	5.97 ± 0.59	5.64 ± 0.11	428 ± 20	340 ± 34

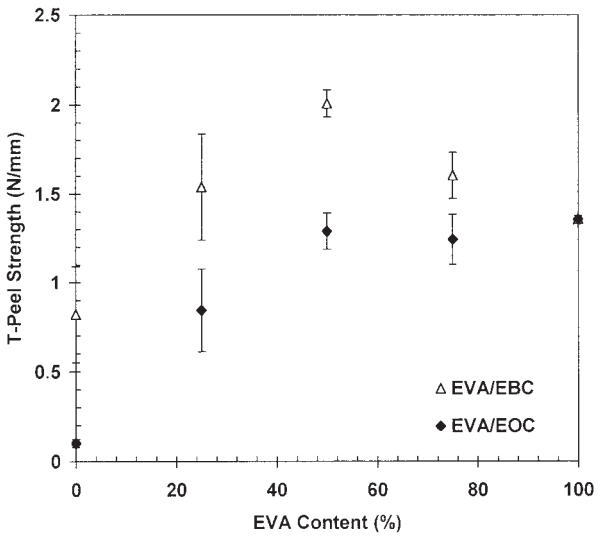

Figure 11 Aluminum T-peel adhesion strength as a function of EVA content.

Adhesive properties

Figure 11 displays the results obtained from the T-peel tests. The mode of failure was adhesive in all cases. As expected, EVA had a higher T-peel strength than either EBC or EOC because of its polar character, which arose from the presence of functional groups. EBC-based blends appeared to be the most beneficial. This may have been because of the higher stiffness of these blends, as evidenced by DMA and tensile testing and/or their lower ΔE, which would facilitate application on the adherent.

A significant synergistic effect was observed for the 50/50 EVA/EBC blend, which may have arisen from the combination of the good adhesive properties of EVA (because of its polarity) and the strength of the EBC.

CONCLUSIONS

Blends of EVA with ultra-low-density ECs were thermodynamically immiscible but compatible, as evidenced by the low values of interfacial tension between the components and their fine morphology and excellent mechanical properties. Synergistic effects were observed in the adhesive and solid-state viscoelastic properties of the blends.

The addition of EVA into the ECs lowered their viscosity at high shear rates, thus improving their processability, but it also resulted in substantial increases in elasticity and η_0. The higher values of the viscoelastic properties of EOC-based blends in the melt state were attributed to the presence of long-chain branching in both EVA and EOC. On the basis of the rheological and morphological analyses and the mechanical property characterizations, it was evident that EVA and EBC were more compatible, which resulted in blends with improved end-use properties.

Support in the form of student scholarships was provided by the Ontario Government and the Natural Sciences and Engineering Research Council of Canada NSERC. T-peel adhesion and optical tests were conducted by J. A. Lee. The authors gratefully acknowledge the contributions of A. M. Henderson and W. E. Baker of AT Plastics, Inc.

References

1. Arsac, A.; Carrot, C.; Guillet, J. J Appl Polym Sci 1999, 74, 2625.
2. Bugada, D. C.; Rudin, A. Eur Polym J 1992, 28, 219.
3. Shimoyama, M.; Hayano, S.; Matsukawa, K.; Inoue, H.; Ninomiya, T.; Ozaki, Y. J Polym Sci Part B: Polym Phys 1998, 36, 1529.
4. Ray, I.; Khastgir, D. Polymer 1993, 34, 2030.
5. Rodríguez-Pérez, M. A.; Duijsens, A.; De Saja, J. A. J Appl Polym Sci 1998, 68, 1237.
6. de Garavilla, J. R. Tappi J 1995, 78, 191.
7. Peón, J.; Vega, J. F.; Aroca, M.; Martínez-Salazar, J. Polymer 2001, 42, 8093.
8. Peón, J.; Aguilar, M.; Vega, J. F.; del Amo, B.; Martínez-Salazar, J. Polymer 2003, 44, 1589.
9. Peón, J.; Vega, J. F.; del Amo, B.; Martínez-Salazar, J. Polymer 2003, 44, 2911.
10. Kontopoulou, M.; Huang, L. C.; Lee, J. A. Adv Polym Technol 2003, 22, 209.
11. Ramírez-Vargas, E.; Navarro-Rodríguez, D.; Medellín-Rodríguez, F. J.; Huerta-Martínez, B. M.; Lin, J. S. Polym Eng Sci 2000, 40, 2241.
12. Gupta, A. K.; Ratnam, B. K.; Srinivasan, K. R. J Appl Polym Sci 1992, 45, 1303.
13. Gupta, A. K.; Ratnam, B. K.; Srinivasan, K. R. J Appl Polym Sci 1992, 46, 281.
14. Ray, I.; Khastgir, D. J Appl Polym Sci 1994, 53, 297.
15. Mishra, S.; Balakrishnan, S.; Chandra, R. J Appl Polym Sci 1998, 70, 1829.
16. Ghosh, M. K.; Das, C. K.; Shingankuli, V. L. Int J Polym Mater 1993, 23, 27.
17. Dealy, J. M.; Wissbrun, K. F. Melt Rheology and Its Role in Plastics Processing; Kluwer Academic: Boston, 1999.
18. Mavridis, H.; Schroff, R. N. Polym Eng Sci 1992, 32, 1778.
19. Utracki, L. A. Polymer Alloys and Blends: Thermodynamics and Rheology; Hanser: Munich, 1990.
20. Carreau, P. J.; DeKee, D. C. R.; Chhabra, R. P. Rheology of Polymer Systems: Principles and Applications; Hanser: Munich, 1997.
21. Lacroix, C.; Aressy, M.; Carreau, P. J. Rheol Acta 1997, 36, 416.
22. Yousefi, A. A.; Ait-Kadi, A.; Roy, C. Adv Polym Technol 1998, 17, 127.
23. Ferry, J. D. Viscoelastic Properties of Polymers; Wiley: New York, 1980.
24. Palierne, J. F. Rheol Acta 1990, 29, 204.
25. Graebling, D.; Muller, R.; Palierne, J. F. Macromolecules 1993, 26, 320.
26. Simanke, A. G.; Galland, G. B.; Freitas, L.; da Jornada, J. A. H.; Quijada, R.; Mauler, R. S. Polymer 1999, 40, 5489.